DEVELOPMENT OF A DAYTIME POLAR CLOUD MASK USING THEORETICAL MODELS OF NEAR- INFRARED BIDIRECTIONAL REFLECTANCE FOR ARM AND CERES

Qing Trepte, Robert F. Arduini, Yan Chen, Sunny Sun-Mack
Science Applications International Corporation, Hampton, VA 23666

Patrick Minnis
Atmospheric Sciences, NASA Langley Research Center, Hampton, VA 23681

Douglas A. Spangenberg, David R. Doelling
AS&M, Inc., Hampton, VA 23666

Proceedings of
AMS 6th Conference on Polar Meteorology and Oceanography
4-18 May 2001
San Diego, CA
pp. 242-245

3B.7 DEVELOPMENT OF A DAYTIME POLAR CLOUD MASK USING THEORETICAL MODELS OF NEAR-INFRARED BIDIRECTIONAL REFLECTANCE FOR ARM AND CERES

Qing Trepte, Robert F. Arduini, Yan Chen, Sunny Sun-Mack
Science Applications International Corporation, Hampton, VA 23666

Patrick Minnis
Atmospheric Sciences, NASA Langley Research Center, Hampton, VA 23681

Douglas A. Spangenberg, David R. Doelling
AS&M, Inc., Hampton, VA 23666

1. INTRODUCTION

Scene identification in satellite imagery over polar regions is difficult because clouds are often similar to the underlying surface in terms of temperature and visible (VIS) reflectance. During the day, however, the brightness temperature difference (BTD) between the 3.7 and 11.0-μm channels on many satellites is greater for clouds than for clear snow allowing for discrimination between clouds and snow. This difference is primarily in the reflected solar component of the solar infrared (SIR) 3.7-μm channel. Similarly, clouds are usually more reflective than snow at 1.6 μm, a near-infrared (NIR) channel on several new satellites. Typically, these channels are used for detecting snow based on either reflectance or temperature difference thresholds that are empirically established. While more accurate than using visible or infrared thresholds alone, these empirical NIR or SIR thresholds are less than satisfactory because of their wide variability, especially with viewing and illumination angles. To minimize the need for empirically adjusting the thresholds for a given set of conditions, to reduce the error accrued from using single-value thresholds, and to facilitate more accurate automated scene identification over snow-bound regions, better characterizations of the bidirectional reflectance patterns of snow at 1.6 and 3.7 μm are needed.

This paper examines the use of theoretical models for improving the cloud masks used by the Clouds and Earth's Radiant Energy System (CERES) project and the Atmospheric Radiation Measurements (ARM) Program. Bidirectional reflectance models of snow at NIR and SIR wavelengths are constructed from the radiative transfer calculations. The NIR and SIR models are used together to classify polar scenes observed with the Terra Moderate-Resolution Imaging Spectroradiometer (MODIS). The resulting cloud mask images are compared with those from the empirical polar scene identification. By using reasonably accurate, theoretically based masks for these two wavelengths; it should be possible to consistently detect clouds over the Arctic, Antarctica, and other snow-covered areas using a variety of different satellites.

**Corresponding author address*: Q. Trepte, SAIC, Inc., Hampton, VA 23666; email: q.z.trepte@larc.nasa.gov

2. THEORETICAL MODELS

The theoretical reflectance models for the snow surface at 0.65, 3.75, and 1.6 μm were developed from calculations using an adding-doubling radiative transfer model. The snow surface was approximated as a layer comprising randomly oriented, hexagonal ice crystals having a length to width ratio, L/D of 750 μm/160 μm with an optical depth τ = 1000. The surface reflectances are corrected to obtain the top-of-the-atmosphere reflectances using correlated-*k* distribution absorption coefficients. The model is discussed further by Spangenberg et al. (2001).

3. SCENE ID USING EMPIRICAL METHODS

The current CERES cloud mask consists of a set of cascading threshold tests that ultimately define a pixel as clear, cloudy, or bad data (Trepte et al. 1999). Cloudy pixels are sub-classified as strong, weak, or no retrieval. Sub-categories for clear pixels include strong, weak, snow, aerosol, smoke, fire, glint, or shadow. Because the initial CERES cloud retrievals were performed using data taken between 37°N and 37°S latitudes, snow cover was not a central focus of the mask. With MODIS data taken frequently over the poles, it is necessary to ensure that the mask is operating accurately. The threshold approach uses values primarily based on subjective examination of high-resolution imager data followed by application and iteration on the values. The thresholds are fixed regardless of viewing geometry.

Figure 1 summarizes the cloud detection process which starts by comparing the observed *BTD* against a set of thresholds. Cloud detection is automatic if *BTD* exceeds 18 K. Otherwise, a second tier of tests uses the ratio of the 1.6 and 0.65-μm reflectances R_{NIR} to detect low and mid-level clouds. If R_{NIR} falls outside the expected range for clouds, then a cold-cloud test is applied. If still not classified as cloudy, the values of R_{NIR}, the ratio of VIS to SIR reflectances R_{SIR}, and the VIS reflectance ρ_V are tested to determine if the pixel is snow/ice. Failing that test, the scene is classified as clear land or ocean or as unknown. The thresholds were determined using a first guess and then iterating on large satellite datasets to obtain stable values.

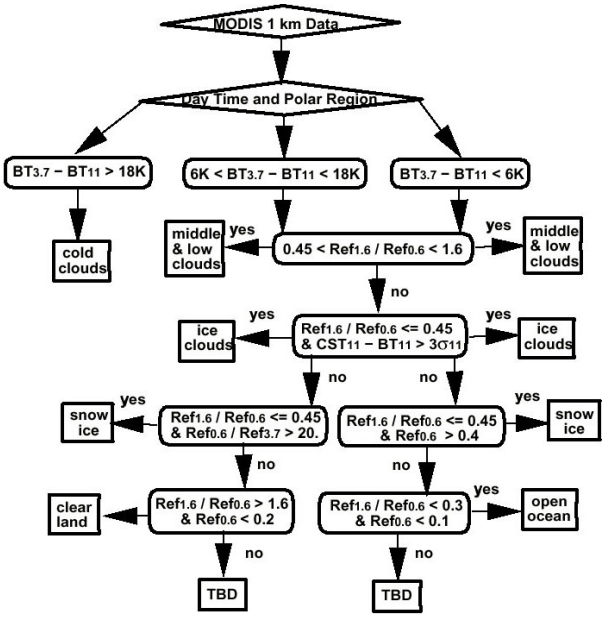

Fig. 1. Flow chart of empirical polar mask.

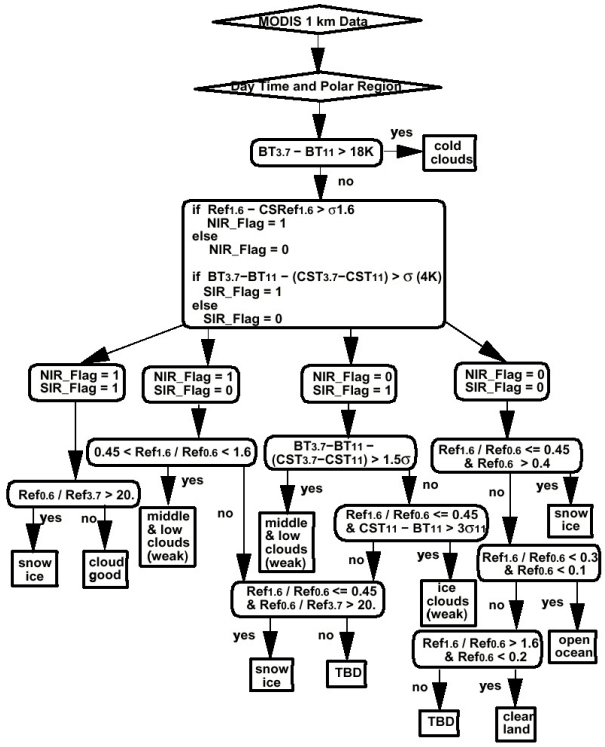

Fig. 2. Flow chart for model-based polar mask.

4. SCENE ID USING NIR AND SIR MODELS

The newer mask, summarized in Fig. 2, uses the same 18K threshold as an absolute cloud detector, but then uses the models to compute the clear-sky reflectance ρ_{Ncs} and ρ_{Scs} for the 1.6 and 3.7-µm channels, respectively. The value of ρ_{Scs} is then used with the 11-µm temperature and sounding to derive the expected clear-sky temperature over snow at 3.7 µm. This value is then used with the expected clear-sky 11-µm temperature to derive a clear-sky brightness temperature difference BTD_{cs}. The difference between the observed BTD and the BTD_{cs} is allowed to be less than one standard deviation σ that is currently fixed at 4K. The pair of tests results in four possible conclusions that are used to select additional tests (see Fig. 2) to arrive at one the final scene classification. Both the old and new algorithms use a thin cirrus test, based on the BTD between the 11 and 12-µm temperatures, that is part of the standard CERES cloud mask. This new technique differs from that of Spangenberg et al. (2001) in that it uses expected model values from 0.65, 1.6, and 3.7-µm snow bidirectional reflectance models and depends more on the BTD than on ρ_S, the 3.7-µm reflectance.

5.0 RESULTS

Both algorithms were applied to eight 5-minute swaths of MODIS data taken during September and October 2000 over either Greenland and surrounding area or over Antarctica including some coastal areas. The standard CERES mask is used unless the solar zenith angle SZA is less than 82° and either the latitude is poleward of 60° or 70°, depending on season, or the surface type is permanent snow cover. The 60° cutoff is used from Nov. through Apr and from May through Oct. for the northern and southern hemispheres, respectively. Preliminary assessment of the MODIS 3.7-µm channel indicates that its brightness temperatures T_S are overestimated by ~2 K. Therefore, all observed T_S values are reduced by 2 K.

Figure 3 shows the results for a swath over Greenland taken 7 September 2000. Part of the scene has SZA > 82° (upper right) and most of the area is south of 70°N. Thus, the polar masks are applied only to the Greenland interior. The darkest areas in both images are classified as clear areas by both masks. The model-based mask detects more cloudiness over western Greenland corresponding to brighter areas in the BTD image. The combined standard and model-based polar mask results are shown at the bottom of figure. An example of the masks applied over Antarctica is shown in Fig. 4. In this case, both masks produce nearly identical results with just slightly more clouds in some areas being found with the model mask. The results in these two figures are typical for all of the swaths examined so far indicating that the model-dependent thresholds are detecting as many as or more clouds than the fixed threshold method.

The mean values of ρ_S and ρ_N for all of the clear snow pixels as identified by the model-based mask were computed for each 5° interval of viewing zenith angle VZA to determine how closely the resulting values compared with the model results. The relative azimuth angles in all of these cases vary from 40° to 140°, so there are pixels with geometry near the principal solar plane. The SZAs range between 56° and 82°. Figure 5

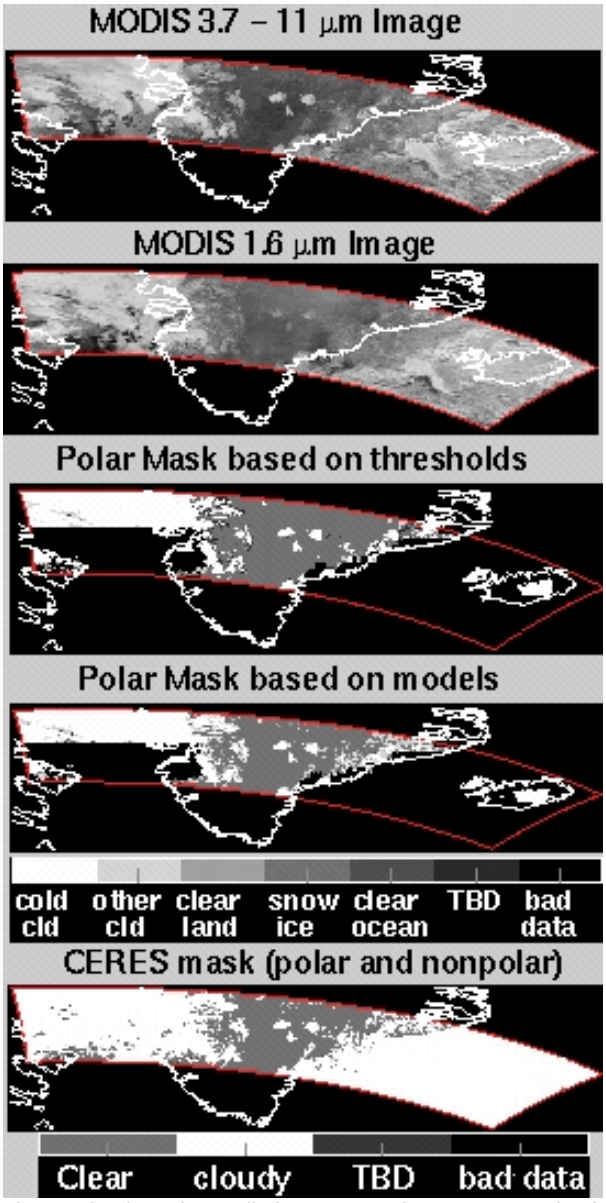

Fig. 3. Cloud masks applied to MODIS data over Greenland, 1435 UTC, 7 September 2000.

shows an example of the mean model and observed NIR reflectances for the case in Fig. 4 using only those VZA bins with more than 5000 pixels. The model and data are in good agreement for most VZAs but diverge at 10° and 47°. The observations are ~3% less on average than the model predicted values and the differences have a standard deviation STD of ~15%. The agreement for the other cases is either as good or worse than that seen here. The typical pattern is an underestimate by the model at small VZAs and an overestimate at greater VZAs. Some of the other cases produce noisier differences

A comparison of model and observed NIR reflectances is shown in Fig. 6 for the same case. There is little agreement between the model and observations.

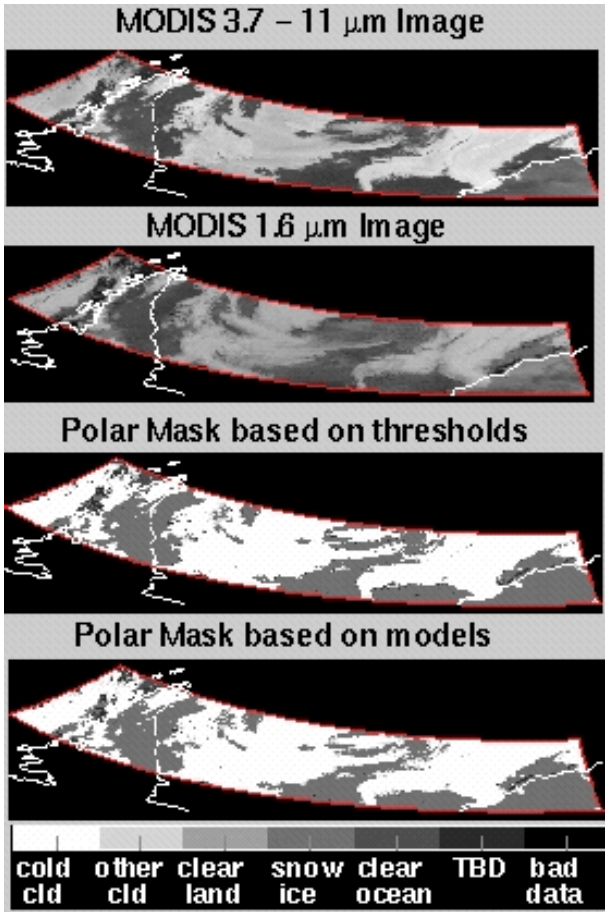

Fig. 4. Same as Fig. 3 except over the Weddell Sea and Antarctica, 1215 UTC, 30 October 2000.

The observed reflectances decrease slightly with VZA while the model values increase significantly. The mean observed reflectances are ~40% less than model values the standard deviation of the differences is 30%. The decrease of p_N with VZA was observed in most of the cases studied here. Thus, the mean value of p_N for all of the cases was ~30% less than the model values although observed reflectances near nadir were sometimes greater than the model estimates.

The behavior of the observed 1.6-μm reflectances is surprising given the few observations of bidirectional reflectance at 1.6 μm over snow-covered surfaces. For example, Arnold et al. (2000) measured the reflectance field from an airplane over snow-covered tundra and sea ice at SZA = 65°. For the angles considered here, they found that the 1.64-μm reflectance increased monotonically from a mean value 0.12 at nadir to 0.14 at 30° up to as high as 0.40 at 70°. The MODIS results have just the opposite behavior suggesting that snow fields can have a wide variety of reflectance patterns. The Arnold et al (2000) data are also not symmetric with relative azimuth angle indicating preferred orientation of the snow surface morphology. The magnitude of the model reflectances are also somewhat greater relative to the Arnold results indicating that a larger ice crystal

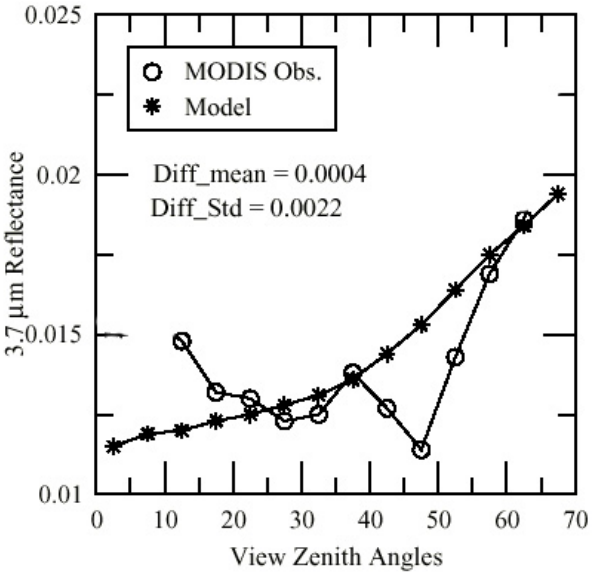

Fig. 5. Comparison of mean model and clear-sky snow 3.7-µm reflectances for data in Fig. 4.

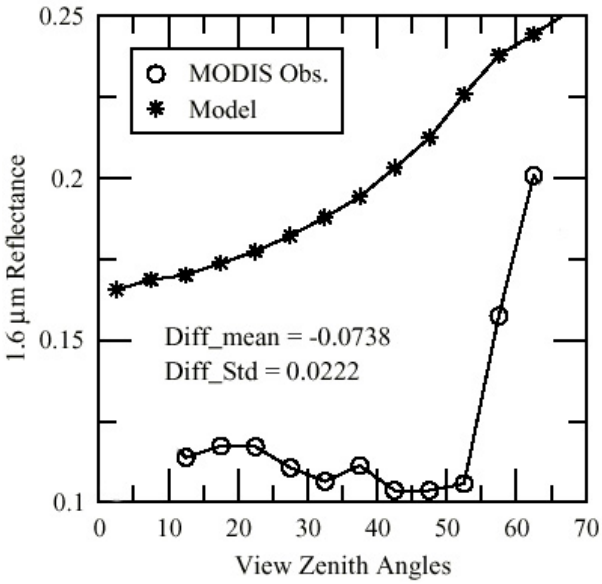

Fig. 6. Comparison of mean model and clear-sky snow 1.6-µm reflectances for data in Fig. 4.

may be required to obtain more realistic values for 1.6 µm snow reflectances.

Warren et al. (1998) reported that erosional features in the snow, sastrugi, in areas like the Antarctic cause more absorption of visible wavelengths by the snow, an effect that may also reduce the reflectance of snow at 1.6 µm as the VZA increases. Sastrugi also have preferred orientations and therefore would introduce asymmetry into a bidirectional reflectance pattern. Thus, much of the scatter and some of the bias seen here may be due to surface effects. The larger part of the bias is probably due to the crystal size used in the calculations.

Spangenberg et al. (2001) found relatively good agreement between the 3.7-µm reflectance model used here and well-characterized clear polar ice scene reflectances. They also found that small amounts of haze or fog may dramatically increase the 3.7-µm reflectance. Therefore, any scenes containing haze or fog would cause overestimates of the reflectances relative to a model value without haze. Similar reflectance increases would be expected at 1.6 µm. Spangenberg et al. also sampled different parts of the relative azimuth domain, so their findings may not be directly applicable to the current study. Another likely source of the model-observation disagreements at 3.7 µm is the uncertainty in the calibration.

6.0 CONCLUDING REMARKS

A model-based and empirical polar cloud mask were found to produce similar cloud amounts although the model reflectance fields were often quite different from the observed values over snow. Much additional study is needed to develop more realistic snow reflectance patterns at various wavelengths. An accurate determination of the MODIS calibrations is also need to understand the amount of error from the calibrations.

Acknowledgements

We would like to thank Sharon Gibson for help with the graphical display software. This research was supported by the NASA Earth Sciences Enterprise CERES Project and Environmental Sciences Division of the DOE ARM Program Interagency Agreement DE-AI02-97ER62341

REFERENCES

Arnold, G. T., S.-C. Tsay, M. D. King, J. Y. Li, and P. F. Soulen, 2000. Airborne spectral measurements of surface-atmosphere anisotropy for Arctic sea ice and tundra. *Intl. J. Rem. Sens.*, submitted.

Minnis, P., P. W. Heck, and D. F. Young, 1993: Inference of cirrus cloud properties from satellite-observed visible and infrared radiances. Part II: Verification of theoretical radiative properties. *J. Atmos. Sci.*, **50**, 1305-1322.

Spangenberg, D. A., V. Chakrapani, and D. R. Doelling, P. Minnis, and R. F. Arduini, 2001: Development of an automated Arctic cloud mask using clear-sky satellite observations taken over the SHEBA and the ARM NSA sites. *Proc. AMS 6th Conf. Polar Meteorol.*, San Diego, CA, May 14-28.

Takano, Y. and K. N. Liou, 1989: Radiative transfer in cirrus clouds: I Single scattering and optical properties of oriented hexagonal ice crystals. *J. Atmos. Sci.*, **46**, 3-20.

Trepte, Q., Y. Chen, S. Sun-Mack, P. Minnis, D. F. Young, B. A. Baum, and P. W. Heck, 1999: Scene identification for the CERES cloud analysis subsystem. *Proc. AMS 10th Conf. Atmos. Rad.*, Madison, WI, June 28 – July 2, 169-172.

Warren, S. G., R. E. Brandt, and P. O'R. Hinton, 1998: Effect of surface roughness on bidirectional reflectance of Antarctic snow. *J. Geophys. Res.*, **103**, 25,789-25,807.